Bioscientia Medicina: Journal of Biomedicine and Translational Research
https://bioscmed.com e-ISSN: 2598-0580 Vol. 10, No. 6 (2026)

ORIGINAL ARTICLE

Mechanism-Specific Tear Film Instability Across Diabetic Retinopathy Severity: Fluorescein Break-Up Pattern Classification in Type 2 Diabetes Mellitus

Petty Purwanita[1*], Ramzi Amin[1], Siti Shalihah Ramadhani Novizar[1]

[1] Department of Ophthalmology, Faculty of Medicine, Universitas Sriwijaya/Dr. Mohammad Hoesin Central General Hospital, Palembang, Indonesia

ARTICLE INFO

Article history
Received: April 4, 2026
Accepted: June 1, 2026
Published: June 30, 2026

Keywords:
Diabetic retinopathy
Dry eye syndromes
Tear film instability
Type 2 diabetes mellitus
Fluorescein

**Corresponding author:*
Petty Purwanita
pettypurwanita@yahoo.com
ORCID: 0000-0002-5900-4036

DOI:
https://doi.org/10.37275/bsm.v10i6.1662

ABSTRACT

Background: Diabetic retinopathy and dry eye disease coexist in type 2 diabetes mellitus, yet conventional metrics treat tear film instability as one entity and cannot identify which layer has failed.

Objective: This pilot study asked whether the Asia Dry Eye Society fluorescein break-up pattern classification tracks Early Treatment Diabetic Retinopathy Study (ETDRS) severity.

Methods: Fifteen patients (30 eyes) with type 2 diabetes and any retinopathy grade were enrolled under a quota framework at RSUP Dr. Mohammad Hoesin Palembang, Indonesia, from November 2024 to July 2025. Break-up patterns were classified into five categories under cobalt-blue slit-lamp biomicroscopy on three consecutive observations; Ocular Surface Disease Index (OSDI) and tear break-up time (TBUT) were recorded. Analysis used rank correlation with exact permutation testing, proportional-odds regression and receiver operating characteristic analysis.

Results: Pattern distribution differed across grades (Fisher–Freeman–Halton p = 0.007; Cramér's V = 0.536). Within the aqueous-deficiency pathway, line break progressed to area break (rho = 0.905, 95% CI 0.666–0.975, exact p = 0.002); within the decreased-wettability pathway, dimple break progressed to spot break (rho = 0.824, 95% CI 0.445–0.953, exact p = 0.009). Each one-grade increase multiplied the odds of a more severe pattern 7.442-fold (95% CI 2.555–21.673), and grade discriminated severe-mechanism patterns with an area under the curve of 0.87 (95% CI 0.681–0.955). OSDI and TBUT deteriorated monotonically (both p < 0.001), whereas random break showed no gradient (rho = 0.095, p = 0.618).

Conclusion: Mechanism-specific tear film failure scales with retinopathy severity, supporting fluorescein-based tear film oriented diagnosis in Indonesian practice.

1. Introduction

Diabetes mellitus has become one of the defining chronic disease burdens of the twenty-first century. The International Diabetes Federation estimated that 537 million adults were living with diabetes in 2021 and projected 783 million by 2045, with the steepest relative increases concentrated in low- and middle-income countries of South and Southeast Asia[1,2]. In Indonesia, serial analysis of the national health surveys places adult diabetes prevalence at 10.7% in 2013, 11.8% in 2018 and 11.3% in 2023, so that a stable proportion applied to an ageing and growing population is still producing a rising absolute burden of microvascular complications[1,3]. Diabetic retinopathy (DR) is the most visually consequential of these complications: a systematic review and meta-analysis of population-based data placed the global prevalence at 22.27% among people with diabetes, corresponding to 103.12 million affected individuals in 2020 and a projected 160.50 million by 2045[4]. Diabetic retinopathy is further distinguished as the only major cause of blindness whose age-standardised prevalence rose over the three decades to 2020, a trajectory that runs counter to the global decline achieved for cataract and trachoma[5]. In Indonesia specifically, a prospective cohort of adults with type 2 diabetes mellitus (T2DM) reported an incidence of diabetic retinopathy of 34.6 per 1000 person-years and of blindness of 8.33 per 1000 person-years, with rural residence carrying roughly 2.5-fold the risk of blindness[6].

Retinal microvascular injury, however, is only the most conspicuous part of the ocular phenotype of diabetes. Dry eye disease (DED) accompanies T2DM in a substantially higher proportion than in age-matched non-diabetic populations, with pooled estimates in diabetic cohorts clustering between 27% and 54% against a background population prevalence near 11.6%[7,8]. Meta-analytic evidence identifies diabetes as an independent risk factor for dry eye after adjustment for age and sex, and contemporary lifestyle-focused

consensus work places systemic metabolic disease among the dominant determinants of ocular surface disease[9-11]. Several converging mechanisms explain the association. Chronic hyperglycaemia produces a length-dependent corneal neuropathy with progressive loss of sub-basal nerve fibre density, blunting the afferent limb of the lacrimation reflex; autonomic neuropathy reduces parasympathetic drive to the lacrimal gland; advanced glycation end-products accumulate within lacrimal acinar tissue and drive oxidative stress and acinar apoptosis; conjunctival goblet cells are depleted with consequent reduction of secreted MUC5AC and membrane-associated MUC16; and meibomian acinar dropout alters the lipid layer that retards evaporation[12-17]. These processes are not merely present in diabetes; they scale with disease severity, and patients with proliferative diabetic retinopathy (PDR) have been reported to carry severe dry eye in up to 61.4% of cases[18,19].

A second problem compounds the first: symptom scores under-detect ocular surface disease in exactly the populations most at risk. In a multicentre Malaysian series of glaucoma patients — a group under chronic topical therapy and therefore comparable in exposure to the diabetic clinic population — 90.4% of eyes had an abnormal break-up time yet roughly a third reported no symptoms at all[20]. The clinical problem is that the instruments in routine use cannot say which of these mechanisms is operating in a given eye. Tear break-up time, Schirmer testing and the Ocular Surface Disease Index each quantify how badly the tear film is failing, but none identifies which layer has failed, and all three therefore lead to the same undifferentiated prescription of lubricant drops[21,22]. The Asia Dry Eye Society (ADES) proposed a resolution to this impasse by redefining dry eye around tear film instability and by operationalising the concept of tear film oriented diagnosis (TFOD), in which the morphology of the fluorescein break-up pattern (FBUP) is read as a direct signature of the deficient layer[22]. Five patterns are recognised. Line break and area break arise from aqueous deficiency, of mild-to-moderate and severe degree respectively, in which the tear film thins to the point of rupture along the lower cornea. Dimple break and spot break arise from decreased surface wettability secondary to mucin deficiency, again in graded severity. Random break reflects evaporative dysfunction from an abnormal lipid layer[23,24]. Because each pattern maps onto a distinct molecular deficit, each also maps onto a distinct therapeutic class — aqueous supplementation and punctal occlusion, mucin secretagogues such as diquafosol sodium and rebamipide, or meibomian-directed therapy — a principle formalised as tear film oriented therapy (TFOT)[24,25]. That the distribution of patterns is itself disease-specific rather than random has already been demonstrated outside diabetes: in thyroid eye disease, line break accounted for 51.9% of eyes, no area break was observed at all, and random break segregated with superior limbic keratoconjunctivitis[26].

For a health system such as Indonesia's, the practical attraction of FBUP assessment is that it requires nothing that an ophthalmology clinic does not already own. A sodium fluorescein strip, a slit lamp with a cobalt blue filter and a trained observer are sufficient; no osmometer, interferometer, meibographer or anterior-segment optical coherence tomography is needed[22,27]. RSUP Dr. Mohammad Hoesin Palembang, the tertiary referral hospital for South Sumatra and the teaching hospital of the Faculty of Medicine, Universitas Sriwijaya, receives diabetic patients from across the province, many of whom present with advanced retinopathy after prolonged periods without screening. In this setting, an assessment that converts a two-minute slit-lamp manoeuvre into a mechanism-specific treatment decision has immediate operational value[6].

Despite the maturity of the ADES framework and the abundance of literature documenting an association between DR and DED as global constructs, no published study has systematically examined whether specific FBUP subtypes segregate by ETDRS-classified retinopathy severity. The existing evidence establishes that diabetic eyes have shorter break-up times and greater symptom burden as retinopathy advances, but it stops short of asking the mechanistic question: does the tear film fail differently — not merely more — at each stage of retinal disease[16,18,28]. Answering that question is the precondition for stage-matched tear film oriented therapy. The present pilot study was therefore designed to characterise the distribution of FBUP subtypes across ETDRS severity grades in Indonesian patients with T2DM, to quantify the strength and direction of association within each mechanistic pathway separately, and to establish whether retinopathy grade carries sufficient information to discriminate eyes with severe-mechanism tear film failure.

2. Methods

Study design, setting and reporting

This was a cross-sectional, single-centre pilot study conducted at the Eye Clinic of Dr. Mohammad Hoesin Central General Hospital, Palembang, the tertiary referral hospital for South Sumatra Province and the principal teaching hospital of Faculty of Medicine, Universitas Sriwijaya, Palembang, Indonesia. Recruitment ran from November 2024 through July 2025. The manuscript is reported in accordance with the Strengthening the Reporting of Observational Studies in Epidemiology (STROBE) statement for cross-sectional studies; the participant flow, eligibility filtering and analytic strata are shown in Figure 1. The study was designated a pilot investigation at the protocol stage because no prior data existed on the joint distribution of FBUP subtype and ETDRS grade, so

the effect size used for planning could not be empirically grounded.

The novelty claim made in this paper was scoped by a structured search of PubMed, Scopus and Google Scholar performed in July 2025, combining the terms 'break-up pattern', 'breakup pattern', 'tear film oriented diagnosis' and 'Asia Dry Eye Society' with 'diabetic retinopathy', 'diabetes' and 'ETDRS', without language restriction and without a date limit. The search was not conducted to the standard of a systematic review and is reported here only to define what the claim of priority does and does not assert. Break-up patterns have previously been described in mixed dry eye populations that included patients with diabetes; what the search did not retrieve was any study in which every eye carried both an independently assigned Early Treatment Diabetic Retinopathy Study grade and an independently assigned break-up pattern, analysed as a joint distribution. It is that narrower claim, and only that claim, which is made here.

Participants and eligibility

Consecutive patients aged 18 to 60 years attending the diabetic retinopathy screening service were assessed for eligibility. Inclusion required a diagnosis of T2DM established by World Health Organization criteria and the presence of any grade of diabetic retinopathy on colour fundus photography. Exclusion criteria were selected to remove conditions that independently perturb tear film dynamics and would therefore confound pattern classification: use of any topical ophthalmic medication within the two weeks preceding examination; active ocular infection or corneal pathology; eyelid abnormality capable of altering tear film distribution, including significant blepharitis, entropion, ectropion or lagophthalmos; intraocular or refractive surgery within the preceding three months; a history of Stevens–Johnson syndrome or Bell palsy; and inability to maintain steady fixation for the duration of the break-up observation. Eligibility was applied at the patient level, and both eyes of an eligible patient entered the study when each independently satisfied the ocular exclusion criteria.

Sample size and sampling strategy

The sample size was derived from the Fisher z-transformation for a single correlation coefficient, using the standard expression

$$n = [\,(z_{1-\alpha} + z_{1-\beta}) \div z_r\,]^2 + 3, \quad \text{where} \quad z_r = \tfrac{1}{2} \cdot \ln[\,(1+\rho) \div (1-\rho)\,]$$

in which $z_{1-\alpha}$ and $z_{1-\beta}$ are the standard normal deviates corresponding to the type I and type II error rates and ρ is the anticipated correlation. Assuming a one-sided alpha of 0.05, 90% power and an anticipated Spearman rho of 0.80, the required number of observation units was 11. Recruitment was then expanded well beyond that minimum, to 15 patients contributing 30 eyes, in order to satisfy the quota of at least six eyes in each of the five pattern categories. The assumed correlation was deliberately optimistic: in the absence of any prior estimate, it represented the effect that the investigators judged large enough to justify a definitive study rather than a realistic expectation, and this is the primary reason the investigation is presented as a pilot requiring external validation. For orientation, the same formula with a two-sided alpha of 0.05 and 80% power requires 30 units to detect a moderate correlation of 0.50, and the minimum detectable correlation at 80% power with 30 eyes is 0.492; with the 12 eyes available in each pathway-specific subgroup it rises to 0.732. Recruitment used consecutive sampling within a quota framework that required a minimum of six eyes in each of the five FBUP categories, so that no pattern would be represented by too few observations to estimate a within-category proportion. The consequences of this design choice for external validity are addressed in the Limitations.

One consequence of the quota design deserves to be stated in statistical rather than descriptive terms, because it determines which of the reported quantities are estimable. Sampling was stratified on break-up pattern, which is the dependent variable in most of the analyses that follow. Under outcome-dependent sampling the marginal distribution of the outcome is fixed by design, so quantities that condition on the outcome, or that are invariant to outcome sampling fractions, remain estimable while quantities that depend on the outcome's marginal frequency do not. Odds ratios are invariant and are therefore valid here, as are the Fisher exact tests and the within-pathway rank correlations, which condition on a fixed six-and-six split. The slope of the logistic model is estimable but its intercept is not. Pattern prevalence, the positive and negative predictive values, and any diversity index computed on the pattern distribution are not estimable from this design, and are reported below as descriptions of the sampled eyes rather than as estimates of population quantities.

Ophthalmic examination protocol

All examinations were performed in a fixed sequence designed so that no test could contaminate the one following it. Symptom assessment preceded any ocular manipulation, tear film assessment preceded pharmacological mydriasis, and retinal imaging was performed last. Ambient conditions in the examination room were held at 22 to 25 degrees Celsius with relative humidity between 50% and 60%, and patients rested for at least ten minutes after arrival before testing began.

Symptoms were quantified with the 12-item Ocular Surface Disease Index administered by structured interview in Bahasa Indonesia by a trained examiner, rather than by self-completion, in order to standardise comprehension across a population with heterogeneous literacy. Responses were scored on the conventional 0 to 100 scale, with scores of 13 or above taken to indicate symptomatic ocular surface disease and the mild, moderate and severe bands defined at the standard cut points.

Fluorescein break-up pattern and tear break-up time were assessed together, following the methodology described by the Asia Dry Eye Society and by Yokoi and colleagues[22,23]. A sterile fluorescein sodium strip was moistened with a single drop of preservative-free saline, the excess was shaken off, and the strip was applied to the central inferior conjunctival fornix. The patient performed three complete blink cycles to distribute the dye, then held the eye open while the tear film was observed under cobalt blue illumination with a yellow barrier filter on a Topcon SL-D7 slit lamp at 10-fold magnification. The interval from the last complete blink to the first appearance of a dark break was recorded as the tear break-up time, and the morphology of that first break was recorded as the FBUP. The entire manoeuvre was repeated three consecutive times with a minimum two-minute interval between repetitions; the pattern appearing in at least two of the three observations was accepted as the final classification, and the three break-up times were averaged. Patterns were assigned as line break, indicating mild-to-moderate aqueous deficiency; area break, indicating severe aqueous deficiency; dimple break, indicating mild-to-moderate decreased wettability; spot break, indicating severe decreased wettability; and random break, indicating evaporative dysfunction attributable to lipid layer abnormality[23,24]. Pharmacological mydriasis was then induced with tropicamide 1%, and retinal imaging was performed with the DRI OCT Triton Plus swept-source system (Topcon Corporation, Tokyo, Japan). Diabetic retinopathy was graded on colour fundus photographs according to the Early Treatment Diabetic Retinopathy Study severity scale into mild non-proliferative diabetic retinopathy (NPDR), moderate NPDR, severe NPDR and proliferative diabetic retinopathy, by a single vitreoretinal subspecialist who was not involved in the tear film assessment[29]. Because tear film assessment always preceded mydriasis and retinal grading, the FBUP examiner was necessarily unaware of the final ETDRS grade at the moment of classification.

A word on masking, which this study did not achieve and does not claim. Because tear film assessment always preceded pharmacological mydriasis and retinal imaging, the examiner performing the break-up classification had not seen the fundus photographs on which the grade was assigned. That is a sequencing safeguard, not masking. The examiner worked within a diabetic retinopathy screening service and had access to the referral information and the clinical history, and advanced proliferative disease is frequently apparent from the referral note alone. The two assessments were made by different investigators, but within a three-author single-centre study their practical independence is weaker than formal masking would provide.

Reliability was addressed only within, not between, observers. Each eye was assessed three times in a single session and the pattern appearing in at least two observations was accepted, which controls for the intrinsic variability of a transient phenomenon; all three observations agreed in the great majority of eyes, and the two-of-three rule was invoked only where they did not. No eye was classified independently by a second observer and no recorded video exists, so neither an inter-observer nor an intra-observer kappa can be reported. The same applies to retinopathy grading, for which the standardisation of the Early Treatment Diabetic Retinopathy Study scale provides more external reassurance than exists for break-up pattern classification.

Unit of analysis

The individual eye was the primary unit of analysis, since FBUP, TBUT and ETDRS grade are all eye-level attributes and can differ between fellow eyes of the same patient. Both eyes were included when each met the criteria. Because measurements from paired eyes are correlated, the effective information content of 30 eyes is smaller than that of 30 independent observations; under plausible inter-eye intraclass correlations of 0.5, 0.7 and 0.9 the design effect reduces the effective sample size to about 20, 17.6 and 15.8 units respectively. A sensitivity analysis restricted to one randomly selected eye per patient was therefore pre-specified, and a complementary exhaustive half-sample analysis was added at the analysis stage and is described below.

Because the effective sample size is smaller than the nominal one, every primary interval is reported twice: as computed on the nominal 30 eyes, and widened under an assumed inter-eye intraclass correlation of 0.7. The value of 0.7 is illustrative rather than empirical; published inter-eye correlations for tear break-up time generally fall between about 0.4 and 0.7, and we are not aware of a published estimate for categorical break-up pattern, which is itself worth recording as a gap.

Data provenance and analytic reconstruction

The analyses reported here were performed on the complete cross-tabulation of ETDRS grade against FBUP category, together with the group-wise counts, means and standard deviations for age, OSDI and TBUT, as recorded in the study database. Because the cross-tabulation is a complete joint distribution of two categorical variables, every eye-level categorical analysis reported below — including the rank correlations, the ordinal regression and the receiver operating characteristic analysis — is exactly recoverable from it and involves no imputation. The reconstruction was validated by recomputing every independently tabulated marginal from the reconstructed eye-level vectors; all reproduced exactly, and the pooled moments recovered from the group statistics likewise reproduced the tabulated overall values (age 53.4 years, OSDI 22.47, TBUT 4.97 seconds). For the continuous variables, only group moments were available, so between-grade

comparisons were recomputed by moment-based parametric methods rather than from individual observations; this is stated wherever such a statistic is reported.

Four families of analysis that a reader might reasonably expect were deliberately not performed, because the available data cannot support them without inventing structure that was never measured. First, no multivariable model adjusting for diabetes duration, glycated haemoglobin or concurrent systemic medication was fitted, because those covariates were not recorded. Second, no generalised estimating equation or mixed-effects model with an eye-within-patient random term was fitted, because the eye-to-patient linkage is not available in the analytic dataset and the working correlation structure therefore cannot be specified. Third, no survival or time-to-event analysis was performed, the design being cross-sectional. Fourth, no receiver operating characteristic analysis of OSDI or TBUT as continuous classifiers was performed, since only their group moments exist; the ROC analysis presented uses the exactly recoverable ordinal ETDRS grade as the classifier. These omissions are restated in the Limitations.

The reconstruction rule is stated in full so that a reader can reproduce it. Each cell of the grade-by-pattern table was expanded into as many eye-level records as the cell count, each record carrying that cell's retinopathy grade and break-up pattern; Ocular Surface Disease Index severity category was then assigned within each grade according to the tabulated category counts for that grade. This produces exactly 30 records and no other assignment is compatible with the published margins. All stochastic procedures — the Fisher–Freeman–Halton simulation, the bootstrap resampling and the half-sample enumeration — were run from a fixed seed of 20260810, so every figure reported here is reproducible to the last decimal place.

Statistical analysis

Analyses were performed in Python 3.11 using SciPy 1.17 and statsmodels 0.14, with all random procedures seeded for exact reproducibility. Continuous variables are summarised as mean plus or minus standard deviation and categorical variables as frequency with percentage. Every proportion is accompanied by a 95% Wilson score interval, with Clopper–Pearson intervals computed in parallel as a conservative check.

The omnibus association between ETDRS grade and FBUP category was tested with the Pearson chi-square statistic and, because 100% of expected cell counts fell below five, with a Fisher–Freeman–Halton exact test evaluated by Monte Carlo simulation over 50000 tables with fixed margins. Association strength is reported as Cramér's V with the Bergsma bias correction. Ordinal association was quantified with Kendall's tau-b, Somers' D, the Goodman–Kruskal gamma and Spearman's rho computed on a tear film severity index in which line break, dimple break, area break and spot break occupy ranks one to four; random break was excluded from the ordered index because evaporative dysfunction is not a graded position on either the aqueous or the wettability axis. Monotonic trend across the ordered retinopathy grades was tested with the Jonckheere–Terpstra statistic and, for the binary contrast of severe-mechanism against other patterns, with the Cochran–Armitage trend test.

Pathway-specific analyses treated the aqueous-deficiency pair (line break versus area break) and the decreased-wettability pair (dimple break versus spot break) as separate two-level ordinal outcomes. For each, Spearman's rho was computed against ETDRS grade, with confidence intervals derived from the Fisher z-transformation using the Bonett–Wright standard error for rank correlations, corroborated by a 5000-replicate bootstrap percentile interval. Because the asymptotic p-value is unreliable at these sample sizes, an exact permutation test enumerating all 924 allocations of the severity labels was computed for each pathway. The corresponding early-versus-advanced two-by-two contrasts were tested by Fisher exact test with Haldane–Anscombe corrected odds ratios.

The dose-response relationship was modelled by proportional-odds ordinal logistic regression of the four-level tear film severity index on ETDRS grade entered as a continuous score, reporting the common odds ratio with a Wald interval, the likelihood ratio test, and McFadden and Nagelkerke pseudo R-squared values. A binary logistic model of severe-mechanism pattern on ETDRS grade was fitted in parallel across all 30 eyes and assessed for calibration by a Hosmer–Lemeshow statistic grouped on the four distinct fitted values. Discrimination was quantified by the area under the receiver operating characteristic curve with a DeLong variance estimate and a logit-transformed confidence interval, and the Youden index was used to select the optimal cut point, for which sensitivity, specificity, predictive values, likelihood ratios and Cohen's kappa are reported with Wilson intervals.

Between-grade differences in OSDI and TBUT were evaluated by one-way analysis of variance reconstructed from the group moments, reported alongside the Welch heteroscedastic variant, with eta-squared, omega-squared and epsilon-squared effect sizes and a 90% confidence interval for eta-squared obtained by inversion of the non-central F distribution. A linear polynomial contrast across the equally spaced ordered grades tested for monotonic dose-response. Pairwise contrasts used Welch t-tests with Hedges' g and its standard error, and p-values were adjusted within each outcome family by the Holm step-down procedure. Diversity of the FBUP profile within each grade was summarised by the Shannon index with the Miller–Madow bias correction and a 5000-replicate bootstrap interval, by Pielou's evenness, by the Simpson index and by the Herfindahl–Hirschman concentration index. Observed proportions were benchmarked against published reference proportions

by exact binomial test, reported as both an absolute risk difference in percentage points and a prevalence ratio. All tests were two-sided with alpha set at 0.05, and exact p-values are given to three decimal places.

The hypothesis structure was as follows. Two primary hypotheses were specified before analysis: that retinopathy grade would correlate with severity within the aqueous-deficiency pathway, and that it would correlate with severity within the decreased-wettability pathway. Three secondary hypotheses were specified: that the overall pattern distribution would differ across grades, and that Ocular Surface Disease Index and tear break-up time would each show a monotonic gradient. All remaining analyses reported here — the ordinal and binary regression models, the receiver operating characteristic analysis, the diversity indices, the external benchmarking and the exhaustive half-sample enumeration — were added at the analysis stage and are exploratory. No analysis plan was registered. Multiplicity is controlled by the Holm procedure within each of the two families of six pairwise contrasts; no global correction is applied across the primary, secondary and exploratory analyses, and the exploratory results should be read accordingly.

Two of the pathway contrasts are completely or nearly completely separated, in which case the maximum likelihood odds ratio is infinite and neither an uncorrected estimate nor a Wald interval is meaningful. These contrasts were therefore fitted by Firth's penalised likelihood, which yields a finite and consistent estimate under separation, with intervals obtained by profiling the penalised likelihood rather than from the Wald approximation. For a saturated two-by-two model Firth's penalty is algebraically equivalent to adding one half to each cell, so the point estimate coincides with the Haldane–Anscombe value; the interval, however, differs substantially and is the quantity that should be read.

Two deviations from the original analysis of the continuous outcomes should be noted. First, the between-grade comparisons of Ocular Surface Disease Index and tear break-up time were originally performed as Kruskal–Wallis tests on individual values; because only group moments were available for the present analysis, they are reported here as analysis of variance reconstructed from those moments, and the two are not the same test. The parametric results should be treated as approximations to the rank-based tests. Second, the group standard deviations are markedly heterogeneous — the variance ratio for tear break-up time between mild and severe non-proliferative disease exceeds six — so the Welch heteroscedastic statistic is reported as the primary result and the equal-variance statistic alongside it.

Ethical approval

Ethical approval was obtained from the Ethics Committee, Faculty of Medicine, Universitas Sriwijaya (approval number 1381/UN9.1.DL/KBK.6.1.3/2024). The study adhered to all tenets of the Declaration of Helsinki in its 2013 revision. Written informed consent was obtained from every participant prior to enrolment, after a verbal and written explanation in Bahasa Indonesia of the purpose of the study, the procedures involved, the absence of any additional risk beyond that of routine ophthalmic examination, and the right to withdraw at any time without any effect on clinical care.

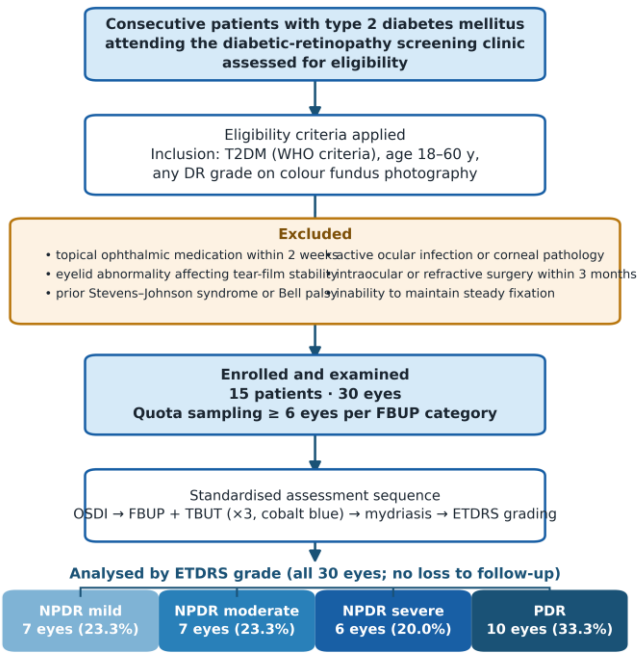

Figure 1. Participant flow through the study, reported according to the Strengthening the Reporting of Observational Studies in Epidemiology (STROBE) statement. Consecutive patients with type 2 diabetes mellitus attending the diabetic retinopathy screening service of Dr. Mohammad Hoesin General Hospital, Palembang between November 2024 and July 2025 were screened against the eligibility criteria shown; 15 patients contributing 30 eyes were enrolled under a quota framework requiring at least six eyes per fluorescein break-up pattern category. All enrolled eyes completed the full assessment sequence, and analytic strata by Early Treatment Diabetic Retinopathy Study grade are shown at the foot of the diagram.

3. Results

Participants and internal consistency of the dataset

Fifteen patients contributing 30 eyes were enrolled and examined; the participant flow is detailed in Figure 1. Mean age was 53.4 plus or minus 6.1 years (median 55, range 43 to 60). Sixteen eyes (53.3%) belonged to female patients and 14 (46.7%) to male patients, corresponding to eight female and seven male participants. Retinopathy grade distribution was mild NPDR in 7 eyes (23.3%, 95% CI 11.8 to 40.9), moderate NPDR in 7 eyes (23.3%), severe NPDR in 6 eyes (20.0%) and PDR in 10 eyes (33.3%, 95% CI 19.2 to 51.2). The predominance of advanced disease reflects the tertiary referral character of the recruiting clinic. Baseline characteristics stratified by retinopathy grade are detailed in Table 1; neither age nor sex differed significantly across grades, and no eye in any grade achieved a normal break-up time, as the final row of Table 1 records.

Table 1. Demographic and baseline characteristics of the study eyes, stratified by Early Treatment Diabetic Retinopathy Study severity grade.

Characteristic	Overall (N = 30 eyes)	NPDR mild (n = 7)	NPDR moderate (n = 7)	NPDR severe (n = 6)	PDR (n = 10)	p-value
Patients, n	15	—	—	—	—	—
Eyes, n (%)	30 (100.0)	7 (23.3)	7 (23.3)	6 (20.0)	10 (33.3)	—
Eyes, % (95% Wilson CI)	—	23.3 (11.8–40.9)	23.3 (11.8–40.9)	20.0 (9.5–37.3)	33.3 (19.2–51.2)	—
Age, years (mean ± SD)	53.4 ± 6.1	55.4 ± 4.4	56.1 ± 4.8	53.3 ± 4.4	50.1 ± 7.7	0.164[a]
Female eyes, n (%)	16 (53.3)	6 (85.7)	1 (14.3)	4 (66.7)	5 (50.0)	0.057[b]
Male eyes, n (%)	14 (46.7)	1 (14.3)	6 (85.7)	2 (33.3)	5 (50.0)	—
Age range, years	43–60	—	—	—	—	—
Eyes with TBUT < 10 s, n (%)	30 (100.0)	7 (100.0)	7 (100.0)	6 (100.0)	10 (100.0)	—

NPDR, non-proliferative diabetic retinopathy; PDR, proliferative diabetic retinopathy; SD, standard deviation; TBUT, tear break-up time; CI, confidence interval. [a] One-way analysis of variance reconstructed from group moments. [b] Fisher–Freeman–Halton exact test by Monte Carlo, used because 88% of expected counts fall below five (Pearson $\chi^2 = 7.71$, $p = 0.052$, Cramér's $V = 0.507$). Proportions of eyes by grade are given with 95% Wilson score intervals. The sex row is tabulated at the eye level throughout; the corresponding patient-level counts are eight female and seven male .

Before inferential analysis, the dataset was audited for internal consistency. Every row of the grade-by-pattern cross-tabulation summed to its stated grade total, every column summed to six eyes as required by the quota design, and the table summed to 30 eyes. Pooled moments recomputed from the group statistics reproduced the tabulated overall values to within rounding for age (53.38 recomputed against 53.4 as published), OSDI (22.47 against 22.46) and TBUT (4.97 against 4.97 seconds); the recomputed values are carried through the manuscript, which is why the overall OSDI appears as 22.47 rather than the published 22.46. A second discrepancy was identified and corrected: the sex row of the original tabulation reported patient-level counts in the overall column while reporting eye-level counts in the grade columns, which is why 16 female eyes are reported here in place of the eight female patients previously tabulated. The percentage is unaffected, since eight of fifteen patients and 16 of 30 eyes both correspond to 53.3%. All eye-level vectors reconstructed from the cross-tabulation reproduced every independently tabulated marginal without residual.

Ocular surface symptoms and tear film stability across retinopathy grades

Ocular surface parameters stratified by retinopathy grade are detailed in Table 2 and displayed in Figure 2. OSDI increased monotonically across the severity spectrum, from 16.83 plus or minus 1.31 in mild NPDR to 26.37 plus or minus 2.12 in severe NPDR and 25.20 plus or minus 2.47 in PDR (Welch $F = 41.418$, $p < 0.001$, the primary test given the unequal group variances; equal-variance $F(3,26) = 13.899$, $p < 0.001$; eta-squared 0.616, 90% CI 0.347 to 0.706; omega-squared 0.563). The linear polynomial contrast across the ordered grades was strongly positive ($t = 6.208$, $p < 0.001$; contrast $r = 0.773$). Tear break-up time fell in mirror image, from 7.43 plus or minus 1.13 seconds in mild NPDR to 3.17 plus or minus 2.79 seconds in severe NPDR and 3.00 plus or minus 2.40 seconds in PDR (Welch $F = 10.232$, $p = 0.001$; equal-variance $F(3,26) =$

8.823, p < 0.001; eta-squared 0.504, 90% CI 0.207 to 0.618; linear contrast t = -4.934, p < 0.001).

Holm-adjusted pairwise contrasts against mild NPDR, as detailed in Table 3 and shown as standardised effect sizes in panel C of Figure 2, quantified the magnitude of these shifts. For OSDI, the mild-to-severe contrast gave a mean difference of -9.54 points (95% CI -11.835 to -7.245) with Hedges' g of -5.142 (95% CI -7.518 to -2.766; Holm-adjusted p < 0.001), and the mild-to-PDR contrast gave -8.37 points (g = -3.81, Holm-adjusted p < 0.001). For TBUT, the mild-to-severe contrast was 4.26 seconds (g = 1.926, Holm-adjusted p = 0.046) and the mild-to-PDR contrast 4.43 seconds (g = 2.111, Holm-adjusted p = 0.001); the complete set of twelve between-grade contrasts, with unadjusted and Holm-adjusted p-values, is given in Table 3. No eye in the entire cohort achieved a tear break-up time of ten seconds or more; the prevalence of an abnormal break-up time was therefore 100% (95% Wilson CI 88.6 to 100). Every eye scored 13 or above on the OSDI and was therefore symptomatic by the conventional threshold; moderate-or-worse symptom burden, defined as an OSDI of 23 or above, was present in 18 eyes (60.0%, 95% CI 42.3 to 75.4), and its distribution across grades followed a significant upward trend (Cochran–Armitage z = 4.018, p < 0.001; Cramér's V = 0.798).

Table 2. Ocular surface parameters and fluorescein break-up pattern distribution, stratified by diabetic retinopathy severity grade.

Parameter	Overall (N = 30)	NPDR mild (n = 7)	NPDR moderate (n = 7)	NPDR severe (n = 6)	PDR (n = 10)	p-value (effect size)
OSDI score, mean ± SD	22.47 ± 4.77	16.83 ± 1.31	20.85 ± 5.26	26.37 ± 2.12	25.20 ± 2.47	<0.001 (η^2 = 0.616)
OSDI below 23 (normal to mild), n (%)	12 (40.0)	7 (100.0)	4 (57.1)	0 (0.0)	1 (10.0)	<0.001 (V = 0.798)
OSDI 23 or above (moderate or severe), n (%)	18 (60.0)	0 (0.0)	3 (42.9)	6 (100.0)	9 (90.0)	—
TBUT, seconds, mean ± SD	4.97 ± 2.93	7.43 ± 1.13	6.86 ± 2.04	3.17 ± 2.79	3.00 ± 2.40	0.001 (η^2 = 0.504)
Line break, n (%)	6 (20.0)	4 (57.1)	2 (28.6)	0 (0.0)	0 (0.0)	0.007 (V = 0.536)
Area break, n (%)	6 (20.0)	0 (0.0)	0 (0.0)	2 (33.3)	4 (40.0)	—
Dimple break, n (%)	6 (20.0)	2 (28.6)	3 (42.9)	1 (16.7)	0 (0.0)	—
Spot break, n (%)	6 (20.0)	0 (0.0)	0 (0.0)	3 (50.0)	3 (30.0)	—
Random break, n (%)	6 (20.0)	1 (14.3)	2 (28.6)	0 (0.0)	3 (30.0)	—
Severe-mechanism pattern (area or spot break), n (%)	12 (40.0)	0 (0.0)	0 (0.0)	5 (83.3)	7 (70.0)	< 0.001[c]

OSDI, Ocular Surface Disease Index; TBUT, tear break-up time; η^2, eta-squared; V, Cramér's V; NPDR, non-proliferative diabetic retinopathy; PDR, proliferative diabetic retinopathy. Continuous variables were compared by the Welch heteroscedastic analysis of variance reconstructed from group moments, which is the primary test because the group variances are markedly unequal; the break-up pattern distribution was compared by Fisher–Freeman–Halton exact test with Monte Carlo evaluation over 50000 tables (Pearson $\chi^2(12) = 25.81$, p = 0.011). [c] Cochran–Armitage test for trend across ordered grades (z = 3.636). Every eye in the cohort scored 13 or above on the OSDI, so all 30 were symptomatic by that threshold; the rows above split the cohort at the moderate cut point of 23.

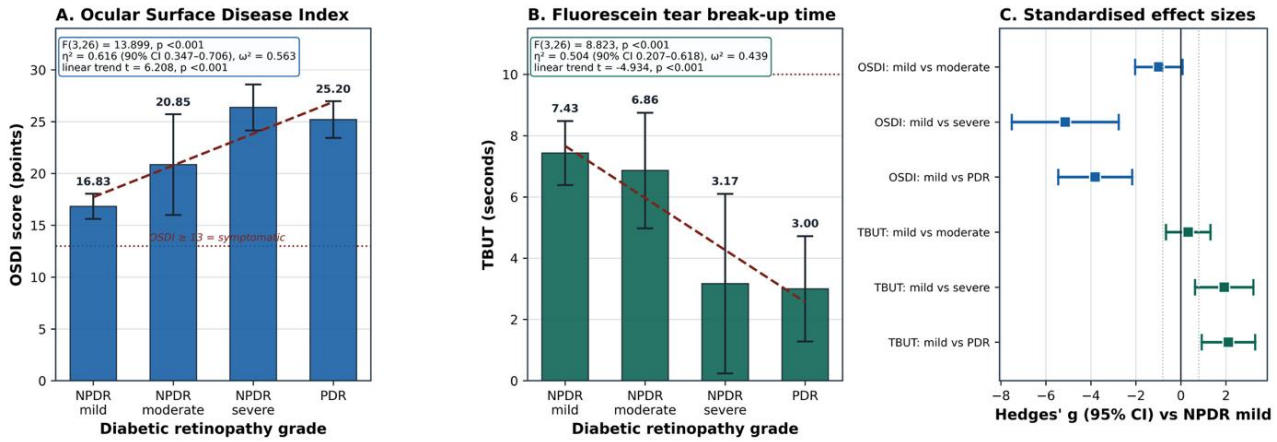

Figure 2. Progressive deterioration of ocular surface parameters across diabetic retinopathy severity grades. Panel A shows Ocular Surface Disease Index scores and panel B tear break-up time, both as group means with 95% confidence intervals, a fitted linear trend and the analysis-of-variance statistics inset; the dotted reference lines mark the symptomatic threshold of 13 points and the normal break-up time of 10 seconds respectively. Panel C presents Holm-adjusted pairwise contrasts against mild non-proliferative disease as standardised effect sizes with 95% confidence intervals.

Distribution of fluorescein break-up patterns

The distribution of break-up patterns differed materially across retinopathy grades, as detailed in Figure 3 and tabulated in the lower block of Table 2. The Pearson chi-square statistic was 25.81 on 12 degrees of freedom (p = 0.011); because all expected cell counts fell below five, the Fisher–Freeman–Halton exact test is the primary result, giving p = 0.007 (Monte Carlo 95% CI 0.007 to 0.008 over 50000 tables). Association strength was moderate to strong, with Cramér's V of 0.536 and a bias-corrected value of 0.407. The composition of that difference was orderly rather than diffuse. In mild NPDR, line break predominated at four of seven eyes (57.1%), consistent with early aqueous deficiency, and no eye showed either of the severe-mechanism patterns. In moderate NPDR, dimple break became the most frequent pattern at three of seven eyes (42.9%), indicating emergent mucin-layer dysfunction, and severe-mechanism patterns remained absent. In severe NPDR, spot break emerged as the dominant finding at three of six eyes (50.0%) and area break appeared in a further two eyes (33.3%). In PDR, area break was the single most common pattern at four of ten eyes (40.0%), with spot break in three (30.0%). Aggregating the two severe-mechanism patterns, their prevalence rose from zero in both mild and moderate NPDR to 12 of the 16 eyes in the advanced grades, a stepwise rise plotted as the overlaid trace in panel B of Figure 3; across the whole cohort 12 eyes (40.0%, 95% CI 24.6 to 57.7) carried a severe-mechanism pattern. The Cochran–Armitage test confirmed a monotonic increase in severe-mechanism prevalence across ordered grades (z = 3.636, p < 0.001).

Table 3. Pairwise between-grade contrasts for ocular surface parameters, with unadjusted and Holm-adjusted significance.

Outcome	Contrast	Mean difference	95% CI	Hedges' g	95% CI	p	Holm p
OSDI	NPDR mild vs NPDR moderate	-4.02	-8.903 to 0.863	-0.982	-2.038 to 0.075	0.092	0.230
OSDI	NPDR mild vs NPDR severe	-9.54	-11.835 to -7.245	-5.142	-7.518 to -2.766	<0.001	<0.001
OSDI	NPDR mild vs PDR	-8.37	-10.35 to -6.39	-3.81	-5.453 to -2.167	<0.001	<0.001
OSDI	NPDR moderate vs NPDR severe	-5.52	-10.505 to -0.535	-1.241	-2.38 to -0.101	0.034	0.136
OSDI	NPDR moderate vs PDR	-4.35	-9.29 to 0.59	-1.076	-2.07 to -0.082	0.077	0.230
OSDI	NPDR severe vs PDR	1.17	-1.369 to 3.709	0.471	-0.502 to 1.443	0.335	0.335
TBUT	NPDR mild vs NPDR moderate	0.57	-1.412 to 2.552	0.324	-0.666 to 1.313	0.533	1.000
TBUT	NPDR mild vs NPDR severe	4.26	1.328 to 7.192	1.926	0.631 to 3.22	0.012	0.046
TBUT	NPDR mild vs PDR	4.43	2.557 to 6.303	2.111	0.923 to 3.299	<0.001	0.001
TBUT	NPDR moderate vs NPDR severe	3.69	0.581 to 6.799	1.424	0.248 to 2.6	0.025	0.075
TBUT	NPDR moderate vs PDR	3.86	1.544 to 6.176	1.619	0.535 to 2.704	0.003	0.015
TBUT	NPDR severe vs PDR	0.17	-2.906 to 3.246	0.063	-0.894 to 1.02	0.904	1.000

OSDI, Ocular Surface Disease Index; TBUT, tear break-up time; CI, confidence interval. Contrasts use Welch t-tests reconstructed from group moments; Hedges' g carries the small-sample correction factor. The Holm step-down adjustment is applied within each outcome family of six contrasts. Omnibus tests: OSDI F(3,26) = 13.899, η^2 = 0.616 (90% CI 0.347–0.706); TBUT F(3,26) = 8.823, η^2 = 0.504 (90% CI 0.207–0.618).

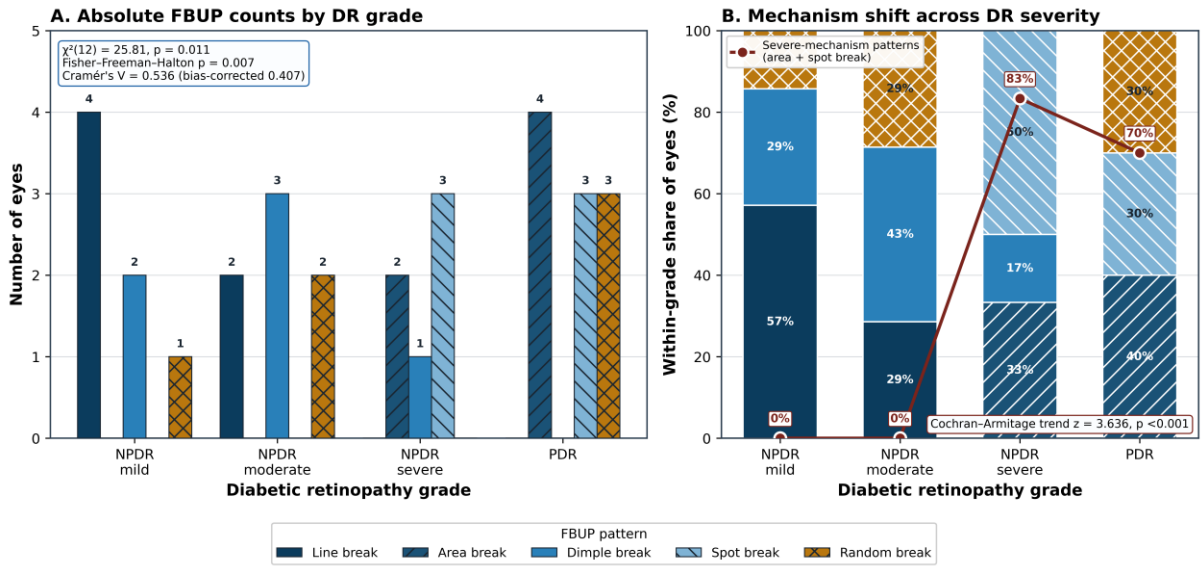

Figure 3. Distribution of fluorescein break-up patterns across diabetic retinopathy severity grades. Panel A shows absolute counts of each pattern within each grade, with the omnibus association statistics inset. Panel B shows the same data as within-grade proportions, overlaid with the prevalence of severe-mechanism patterns (area break plus spot break, dark red line). Line break gives way to area break within the aqueous-deficiency pathway and dimple break to spot break within the decreased-wettability pathway as retinopathy advances, whereas random break shows no ordered progression.

Considered as an ordered severity index across the four mechanistically graded patterns, the association with retinopathy grade was strong and monotone, as detailed in Table 4: Spearman rho was 0.801 (95% CI 0.571 to 0.915, p < 0.001), Kendall's tau-b 0.682, Somers' D 0.684 and the Goodman–Kruskal gamma 0.821, with 163 concordant against 16 discordant pairs. The Jonckheere–Terpstra test for ordered alternatives was highly significant (z = 3.915, p < 0.001). The within-grade profile did not, however, become narrower as retinopathy advanced, as detailed in the lower block of Table 4: exactly three of the five patterns were observed in every grade, the Shannon index moved from 0.956 in mild NPDR to 1.089 in PDR, and the Herfindahl–Hirschman concentration index moved from 4286 to 3400. Neither series is monotonic, and the direction of both is the opposite of concentration: what changes across grades is the composition of the profile, not its breadth.

Two caveats attach to the combined ordered index. First, ranking dimple break above line break and below area break asserts that the aqueous and wettability pathways lie on a common severity scale, which is a clinical assumption rather than an established fact; under the alternative ordering that keeps each pathway intact — line, area, dimple, spot — the correlation falls to 0.442 (p = 0.030), so the strength of the combined index is not robust to this choice and the pathway-specific analyses should be regarded as primary. Second, the proportional-odds assumption underlying the ordinal model was examined by fitting separate binary logistic models at each cut point of the index. Only two of the three cut points yielded an estimable slope, the third being separated; the estimable slopes did not differ significantly (Q = 0.535 on 1 degree of freedom, p = 0.465), but with 24 observations this check has very little power and the assumption is best described as untested rather than satisfied.

Aqueous-deficiency pathway

Among the 12 eyes exhibiting an aqueous-deficiency pattern, segregation by retinopathy grade was complete. Every eye with line break fell in the two earlier grades — four in mild NPDR and two in moderate NPDR — and every eye with area break fell in the two advanced grades, two in severe NPDR and four in PDR. Spearman's rho between retinopathy grade and pattern severity was 0.905 (95% CI 0.666 to 0.975; widened to 0.437 to 0.987 under an assumed inter-eye correlation of 0.7; bootstrap 95% CI 0.73 to 0.977), as detailed in Table 4. Because the asymptotic p-value is not trustworthy at this sample size, an exact permutation test enumerating all 924 label allocations was computed and gave p = 0.002; Fisher's exact test gave p = 0.002. The early-versus-advanced contrast is completely separated, six eyes against six, so the maximum likelihood odds ratio is infinite. Fitted by Firth's penalised likelihood, the odds ratio is 169 with a profile penalised-likelihood 95% interval from 6.7 to 55715. That interval spans nearly four orders of magnitude and should be read as establishing direction, not magnitude. The relationship is displayed in panel A of Figure 4.

Decreased-wettability pathway

Among the 12 eyes exhibiting a decreased-wettability pattern, dimple break accounted for every affected eye in mild and moderate NPDR, while spot break accounted for three of four such eyes in severe NPDR and all three in PDR. Spearman's rho was 0.824 (95% CI 0.445 to 0.953; widened to 0.137 to 0.976 under an

assumed inter-eye correlation of 0.7; bootstrap 95% CI 0.605 to 0.933; exact permutation p = 0.009). This contrast is nearly separated and was likewise fitted by penalised likelihood, giving an odds ratio of 47.7 (profile 95% CI 2.9 to 7830; Fisher exact p = 0.015). The relationship is displayed in panel B of Figure 4, and pathway-specific estimates are collected in Table 4.

Table 4. Rank-correlation, ordinal-association and trend analyses linking diabetic retinopathy severity to fluorescein break-up pattern, and the within-grade concentration of the pattern profile.

Pathway / analysis	Variable pair or statistic	n (eyes)	Statistic	Estimate	95% CI	Bootstrap 95% CI	p-value	Effect / interpretation
Aqueous deficiency	DR grade vs line break → area break	12	Spearman ρ	0.905	0.666–0.975	0.73–0.977	0.002	Large
Aqueous deficiency, ICC 0.7 adjusted	effective n = 7.1	12	Spearman ρ	0.905	0.437–0.987	—	0.002	Large
Decreased wettability	DR grade vs dimple break → spot break	12	Spearman ρ	0.824	0.445–0.953	0.605–0.933	0.009	Large
Decreased wettability, ICC 0.7 adjusted	effective n = 7.1	12	Spearman ρ	0.824	0.137–0.976	—	0.009	Large
Combined ordered index	DR grade vs tear film severity index	24	Spearman ρ	0.801	0.571–0.915	—	<0.001	Large
Combined index, alternative ordering	line, area, dimple, spot	24	Spearman ρ	0.442	—	—	0.030	Medium
Combined ordered index	Kendall's tau-b	24	τ-b	0.682	—	—	<0.001	Large
Combined ordered index	Somers' D (severity | grade)	24	D	0.684	—	—	—	Large
Combined ordered index	Goodman–Kruskal gamma (ties excluded)	24	γ	0.821	—	—	—	Large
Ordered-alternative trend	Jonckheere–Terpstra	24	z	3.915	—	—	<0.001	Monotone
Binary trend	Cochran–Armitage, severe-mechanism pattern	30	z	3.636	—	—	<0.001	Monotone
Evaporative	DR grade vs random break	30	Spearman ρ	0.095	-0.296–0.458	—	0.618	Negligible
Exhaustive half-samples	Aqueous pathway, median of 922 valid subsets	6	Spearman ρ	0.894	0.707–1.000	—	—	Large
Exhaustive half-samples	Wettability pathway, median of 922 valid subsets	6	Spearman ρ	0.853	0.612–0.949	—	—	Large
Within-grade profile concentration								
NPDR mild	Shannon H′ · Miller–Madow 1.099 · Pielou J′ 0.870 · Simpson 0.667 · HHI 4286	7	H′	0.956	0.410–1.079	—	—	S = 3
NPDR moderate	Shannon H′ · Miller–Madow 1.222 · Pielou J′ 0.982 · Simpson 0.762 · HHI 3469	7	H′	1.079	0.410–1.079	—	—	S = 3
NPDR severe	Shannon H′ · Miller–Madow 1.178 · Pielou J′ 0.921 · Simpson 0.733 · HHI 3889	6	H′	1.011	0.451–1.099	—	—	S = 3
PDR	Shannon H′ · Miller–Madow 1.189 · Pielou J′ 0.991 · Simpson 0.733 · HHI 3400	10	H′	1.089	0.639–1.089	—	—	S = 3
All grades combined	Shannon H′ · Miller–Madow 1.676 · Pielou J′ 1.000 · Simpson 0.828 · HHI 2000	30	H′	1.609	—	—	—	S = 5

DR, diabetic retinopathy; CI, confidence interval; ICC, intraclass correlation. p-values for the two primary pathways are exact permutation values enumerating all 924 label allocations. Analytic intervals use the Bonett–Wright standard error for rank correlations; bootstrap intervals use 5000 percentile replicates. Rows marked 'ICC 0.7 adjusted' recompute the interval on the effective sample size implied by an assumed inter-eye correlation of 0.7 (7.1 of 12 eyes). Of the 924 possible six-eye half-samples in each pathway, 2 are degenerate (all eyes sharing one pattern) and Spearman's rho is undefined; the 922 valid subsets are summarised here and every one gave a positive correlation. The alternative ordering row keeps each pathway intact instead of interleaving them, and is reported because the combined index is sensitive to that choice. In the final column, magnitudes for rank correlations follow Cohen's conventions; the trend rows report a direction rather than a magnitude. In the concentration block, H′ is the Shannon index in natural-log units with the Miller–Madow small-sample bias correction given alongside; J′ is Pielou evenness; HHI is the Herfindahl–Hirschman concentration index on the conventional 0–10 000 scale, where higher means more concentrated; S is the number of distinct patterns observed. Three of the five patterns appear in every grade, and neither H′ nor HHI changes monotonically with retinopathy severity — the profile shifts in composition without narrowing. Because the quota design fixed the overall pattern totals at six eyes each, these indices describe the sampled eyes and are not estimates of population diversity.

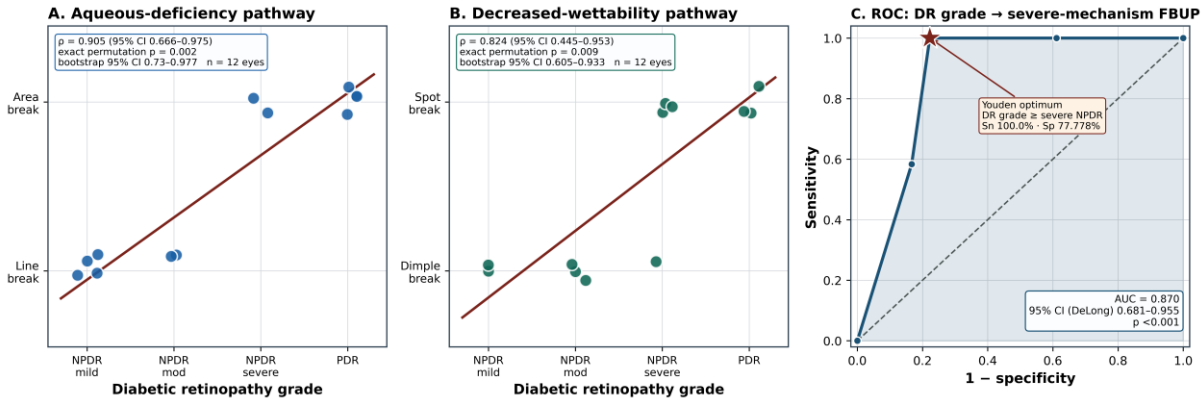

Figure 4. Pathway-specific associations and diagnostic discrimination. Panel A shows the aqueous-deficiency pathway, in which eyes progress from line break to area break with advancing retinopathy grade, and panel B the decreased-wettability pathway, in which dimple break gives way to spot break; both panels are jittered for visibility and annotated with the rank correlation, its analytic and bootstrap confidence intervals and the exact permutation p-value. Panel C shows the receiver operating characteristic curve for retinopathy grade as a classifier of severe-mechanism break-up pattern, with the Youden-optimal cut point starred.

Evaporative pathway

Random break, the signature of evaporative dysfunction, behaved differently from both graded pathways. It was observed in one eye in mild NPDR (14.3%), two in moderate NPDR (28.6%), none in severe NPDR and three in PDR (30.0%). Neither a rank correlation nor a trend test detected any systematic relationship with retinopathy grade, and the concentration indices in the lower block of Table 4 show no narrowing of the pattern profile to accompany it (rho = 0.095, 95% CI -0.296 to 0.458, p = 0.618; Cochran–Armitage z = 0.469, p = 0.639). This null result is quantified rather than merely asserted: with 30 eyes the analysis had 80% power to detect a correlation of 0.492 or larger, so a relationship of moderate strength would probably have been detected had one existed, while weaker associations remain compatible with these data.

Dose-response modelling and diagnostic performance

Proportional-odds ordinal logistic regression of the four-level tear film severity index on retinopathy grade, as detailed in the upper block of Table 5, gave a common odds ratio of 7.442 per one-grade increase (95% CI 2.555 to 21.673, p < 0.001; likelihood ratio chi-square 21.395, p < 0.001; McFadden R-squared 0.322, Nagelkerke R-squared 0.629). The parallel binary logistic model for severe-mechanism pattern across all 30 eyes gave an odds ratio of 5.675 per grade (95% CI 1.787 to 18.021, p = 0.003; Nagelkerke R-squared 0.555). A Hosmer–Lemeshow statistic is reported for completeness (chi-square 5.781 on 2 degrees of freedom, p = 0.056) but is descriptive only: with a single ordinal predictor the fitted probabilities take just four distinct values, so the test has neither its intended decile grouping nor any useful power, and calibration is judged instead from the observed-against-expected block of Table 5.

Discrimination, summarised in the middle block of Table 5, is displayed in panel C of Figure 4. Retinopathy grade separated eyes with and without a severe-mechanism pattern with an area under the curve of 0.87 (DeLong 95% CI 0.681 to 0.955, p < 0.001; bootstrap 95% CI 0.727 to 0.986 over 10000 replicates). Because the classifier takes only four distinct values the empirical curve has four points and the tie structure is heavy, so the bootstrap interval is the more trustworthy of the two. The Youden-optimal cut point was a grade of severe NPDR or worse, at which sensitivity was 12 of 12 (100%, 95% CI 75.8 to 100) and specificity 14 of 18 (77.8%, 95% CI 54.8 to 91.0), with a positive likelihood ratio of 4.5, overall accuracy 86.7% and Cohen's kappa 0.737. Calibration is shown directly in Table 5 as observed against expected counts at each grade.

The predictive values require an explicit warning. Positive and negative predictive value both depend on the prevalence of the condition being classified, and the prevalence of severe-mechanism patterns in this cohort — 40.0% — is fixed by the quota design rather than estimated. Within the sampled eyes the positive predictive value was 75.0% and the negative predictive value 100%. Applying the same sensitivity and specificity at a severe-mechanism prevalence of 20%, which is closer to what a screening population might carry, the positive predictive value falls to 52.9% while the negative predictive value remains 100%; at a prevalence of 10% the positive predictive value falls further, to 33.3%. Sensitivity and specificity are prevalence-invariant and can be carried across settings; the predictive values cannot.

Table 5. Dose-response modelling, diagnostic performance, omnibus association, and external benchmarking of the cohort against published reference proportions.

Model / statistic	Estimate	95% CI	p-value	Model metric
Proportional-odds ordinal logistic regression				
DR grade (per one-grade increase)	OR 7.442	2.555–21.673	<0.001	Nagelkerke R^2 0.629
Model likelihood ratio test	$\chi^2(1) = 21.395$	—	<0.001	McFadden R^2 0.322
Binary logistic regression — severe-mechanism pattern				
DR grade (per one-grade increase)	OR 5.675	1.787–18.021	0.003	Nagelkerke R^2 0.555
Hosmer–Lemeshow goodness of fit	$\chi^2(2) = 5.781$	—	0.056	Descriptive only; 4 fitted values
Penalised-likelihood odds ratios (separated contrasts)				
Aqueous pathway, early vs advanced DR	OR 169.0	6.7–55715.0	0.002	Firth; complete separation
Wettability pathway, early vs advanced DR	OR 47.7	2.9–7830.0	0.015	Firth; near separation
Discrimination — DR grade as classifier				
Area under the ROC curve	AUC 0.87	0.681–0.955[a]	<0.001	SE 0.066
Youden-optimal cut point (≥ severe NPDR)	J = 0.778	—	—	Accuracy 86.7%
Sensitivity	100.0%	75.8–100.0	—	TP 12, FN 0
Specificity	77.8%	54.8–91.0	—	TN 14, FP 4
Positive predictive value	75.0%	50.5–89.8	—	LR+ 4.5
Negative predictive value	100.0%	78.5–100.0	—	LR− 0.0
Agreement with severe-mechanism status	κ = 0.737	—	—	Substantial
Omnibus association — grade × pattern				
Pearson chi-square	$\chi^2(12) = 25.81$	—	0.011	Cramér's V 0.536
Fisher–Freeman–Halton exact (Monte Carlo)	—	0.007–0.008[b]	0.007	Bias-corrected V 0.407
Cochran–Armitage trend	z = 3.636	—	<0.001	Monotone increase
Jonckheere–Terpstra trend	z = 3.915	—	<0.001	Ordered alternative
Predictive value at a lower severe-mechanism prevalence				
PPV at 20% prevalence	52.9%	—	—	NPV 100.0%
PPV at 10% prevalence	33.3%	—	—	NPV 100.0%
Calibration — observed vs expected severe-mechanism eyes				
NPDR mild (n = 7)	observed 0	expected 0.174	—	difference -0.17
NPDR moderate (n = 7)	observed 0	expected 0.885	—	difference -0.89
NPDR severe (n = 6)	observed 5	expected 2.706	—	difference +2.29
PDR (n = 10)	observed 7	expected 8.234	—	difference -1.23
External benchmarking (exact binomial test)				
Abnormal tear break-up time (< 10 s) — 30/30 vs 54.0% (upper bound of the pooled dry eye prevalence in type 2 diabetes (Chen et al., systematic review and meta-analysis))	100.0%	88.6–100.0	<0.001	RD +46.0 pp; PR 1.852
Moderate-or-worse OSDI (≥ 23) — 18/30 vs 41.8% (dry eye prevalence in type 2 diabetes, Indian cross-sectional cohort (Prasad et al.))	60.0%	42.3–75.4	0.062	RD +18.2 pp; PR 1.434

OR, odds ratio; ROC, receiver operating characteristic; AUC, area under the curve; TP/FP/TN/FN, true and false positives and negatives; LR+/LR−, positive and negative likelihood ratios; κ, Cohen's kappa; DR, diabetic retinopathy; NPDR, non-proliferative diabetic retinopathy. The ordinal outcome is the tear film severity index (line break 1, dimple break 2, area break 3, spot break 4); random break is excluded from the ordered index. [a] DeLong variance with logit-transformed interval. [b] Monte Carlo simulation interval for the exact p-value. Proportions carry 95% Wilson score intervals. Odds ratios for the two pathway contrasts are Firth penalised-likelihood estimates with profile penalised-likelihood intervals, because both contrasts are separated and the maximum likelihood estimate is infinite. The Hosmer–Lemeshow statistic is reported descriptively only; the calibration block below it shows observed against expected counts directly. The AUC bootstrap interval is 0.727–0.986 over 10000 replicates and is preferred to the DeLong interval given the heavy tie structure. In the benchmarking block the Estimate column is the observed percentage, the interval is its 95% Wilson score interval, the p-value is an exact binomial test against the stated reference, and RD and PR are the absolute risk difference in percentage points and the prevalence ratio. Two qualifications apply: the reference proportions come from mixed community and clinic samples across several countries whereas this is a quota sample from a single tertiary referral clinic, so these rows quantify a discrepancy from a non-comparable reference rather than testing a hypothesis; and the reference is treated as a constant known without error, so the intervals propagate uncertainty in the present cohort only and are anticonservative. The two rows also measure different constructs — an objective sign against a pooled prevalence, and a symptom band against a clinical diagnosis. A third comparison, against the distribution expected if all five patterns were equally frequent, was withdrawn because the quota design forces the observed distribution close to uniform and the comparison would test the design, not the biology.

Sensitivity analyses and external benchmarking

The pre-specified sensitivity analysis restricted to one randomly selected eye per patient was recorded in the source dataset as rho = 0.89 for the aqueous pathway and rho = 0.79 for the decreased-wettability pathway, preserving both the direction and the magnitude of the primary correlations. Those coefficients could not be recomputed here, because the eye-to-patient linkage is not present in the analytic dataset, and no p-value is quoted for them: with six observations and a two-level split an exact permutation test admits only twenty arrangements, so the smallest attainable two-sided p-value is 0.100 and any smaller value would be unattainable by construction. In place of that analysis an exhaustive half-sample procedure was run, in which every one of the 924 possible six-eye subsets of each pathway was evaluated. Two subsets in each pathway are degenerate, containing a single pattern, so Spearman's rho is undefined for them; across the 922 valid subsets the median correlation was 0.894 for the aqueous pathway (2.5th to 97.5th centile 0.707 to 1.000) and 0.853 for the wettability pathway (0.612 to 0.949), and every valid subset yielded a positive correlation. The association is therefore not an artefact of any particular eye selection. The external comparisons that follow are collected in the lower block of Table 5.

Benchmarking against published reference proportions, as detailed in the lower block of Table 5, places the cohort in international context, with two important qualifications. The reference proportions are drawn from mixed community and clinic samples across several countries, whereas this is a quota sample from a tertiary referral clinic in equatorial Indonesia, so the comparison quantifies a discrepancy from a non-comparable reference rather than testing a hypothesis; and the reference is treated as a constant known without error, so the intervals propagate uncertainty in the present cohort only. With those caveats, the prevalence of an abnormal tear break-up time, at 100%, exceeds the upper bound of the pooled dry eye prevalence reported for type 2 diabetes by 46.0 percentage points (prevalence ratio 1.852)[7], and moderate-or-worse symptom burden at 60.0% exceeds the 41.8% dry eye prevalence reported in an Indian type 2 diabetes cohort by 18.2 percentage points[30]. A third comparison, against the distribution expected if all five patterns were equally frequent, was dropped from this analysis because the quota design forces the observed distribution close to uniform and the comparison would therefore test the design rather than the biology.

Finally, the point estimates reported here should be read as upper bounds. Effect estimates conditional on having reached statistical significance in small samples are systematically inflated, and no shrinkage model can be fitted from a single sample. The defensible planning value is therefore the lower bound of the interval rather than the point estimate: 0.666 for the aqueous pathway and 0.445 for the decreased-wettability pathway. Powered on those values at 80% power and a two-sided alpha of 0.05, a definitive study would require 16 and 38 eyes respectively, against the 12 available in each pathway here — roughly a third more for the aqueous pathway and about three times as many for the decreased-wettability pathway. Both figures are per pathway. Each pathway accounted for 12 of the 30 eyes, so the binding requirement — 38 decreased-wettability eyes — implies a total enrolment of about 95, which is where the recommendation of at least 100 eyes below comes from.

4. Discussion

This pilot study is, to our knowledge, the first to test whether the specific morphology of tear film break-up — rather than its mere presence or duration — tracks the severity of diabetic retinopathy. The answer, in this cohort of 30 eyes examined at RSUP Dr. Mohammad Hoesin Palembang, is that it does, and that it does so along two mechanistically separable axes while leaving a third untouched. Within the aqueous-deficiency pathway, progression from line break to area break tracked retinopathy grade with rho = 0.905 (exact p = 0.002); within the decreased-wettability pathway, progression from dimple break to spot break tracked it with rho = 0.824 (exact p = 0.009). Considered as a single ordered severity index, each additional retinopathy grade multiplied the odds of a more severe pattern by 7.442 (95% CI 2.555 to 21.673), and retinopathy grade discriminated severe-mechanism failure with an area under the curve of 0.87. Random break, by contrast, showed no gradient whatsoever. That dissociation is the study's central observation: it is precisely what one would predict if the aqueous and mucin pathways are driven by the same systemic microvascular and neuropathic processes that damage the retina, while the evaporative pathway is governed by lid-margin factors that operate independently of glycaemic burden.

A rival explanation must be confronted before any mechanistic reading is offered. Retinopathy grade is, to a first approximation, a function of diabetes duration and cumulative glycaemic exposure; so is diabetic corneal neuropathy, and so is conjunctival goblet-cell loss[12,16,31]. The association reported here is therefore entirely compatible with retinal and ocular surface disease being parallel consequences of the same antecedent metabolic exposure, with no direct relationship between them at all. Because diabetes duration and glycated haemoglobin were not recorded, this study cannot distinguish shared antecedent causation from a specific retina-to-surface relationship. That distinction matters for the mechanistic claim but not for the clinical one: as a triage rule, the observation that advanced retinopathy identifies eyes with severe-mechanism tear film failure is useful whether the relationship is direct or shared. The language

throughout this discussion is chosen to preserve that separation.

The aqueous-deficiency finding sits alongside a small but consistent literature on graded ocular surface change in diabetes. A pooled meta-analysis of 24 observational studies found shorter invasive and non-invasive break-up times, lower Schirmer values and higher symptom scores in type 2 diabetes than in non-diabetic controls[10]. Machaliańska and colleagues went further and showed that retinopathy stage correlates with corneal nerve loss and with symptom burden even where Schirmer, non-invasive break-up time and tear meniscus height do not differ — which is precisely the situation in which a mechanism-specific reading of the break-up pattern adds information that conventional signs cannot[18]. The mechanistic explanation is now reasonably well characterised. Corneal sub-basal nerve fibre density declines in proportion to systemic neuropathy severity, degrading the afferent limb of the lacrimation reflex, while autonomic neuropathy attenuates parasympathetic secretory drive[12,32]. In parallel, advanced glycation end-products accumulate within lacrimal acinar tissue, where they generate reactive oxygen species and precipitate acinar apoptosis; this has been demonstrated both in human ocular surface tissue and in experimental models of type 2 diabetes[14,15]. The magnitude of the correlation observed here suggests that the degree of aqueous deficiency legible at the slit lamp is a reasonably faithful surrogate for the extent of the same microvascular and neuropathic injury that produces retinopathy.

The decreased-wettability finding carries a different and arguably more clinically actionable implication. Spot break, the signature of severe mucin deficiency, was confined entirely to eyes with severe NPDR or PDR. Chronic hyperglycaemia induces apoptosis of conjunctival goblet cells and downregulates both the secreted mucin MUC5AC and the membrane-associated mucin MUC16, the latter of which constitutes the glycocalyx barrier that renders the corneal epithelium wettable[16,33]. Experimental work has shown that loss of membrane-associated mucin precedes measurable epithelial barrier breakdown, which positions spot break as a potentially early warning of surface decompensation rather than a late consequence of it[33]. If that sequence holds prospectively, the appearance of spot break in a diabetic eye would warrant mucin-directed therapy before corneal staining becomes apparent — a meaningfully earlier intervention point than current practice offers.

The absence of any retinopathy gradient for random break is equally informative and deserves emphasis rather than dismissal as a negative result. Meibomian gland dysfunction in diabetes has repeatedly been shown to relate to age, sex, environmental exposure and blink dynamics rather than to retinal disease stage, and lipid layer thickness in diabetic eyes appears to be governed by meibomian rather than retinal burden[17,34]. Meibomian dropout is in fact detectable in type 2 diabetes even when glycaemia is well controlled and the patient is asymptomatic, which is exactly the profile of a process running on its own clock[35]. The present data are consistent with that literature, and the analysis was adequately resolved to make the statement meaningful: with 30 eyes there was 80% power to detect a correlation of 0.492, so a moderate association would probably have been visible. Practically, this means that retinopathy grade should not be used as a proxy for evaporative risk; an eye with mild NPDR may carry substantial meibomian disease, and lid assessment cannot be omitted merely because the retina looks reassuring.

The statistical magnitude of the ocular surface gradients should be translated into clinical terms, because effect-size conventions borrowed from psychology carry no meaning at a slit lamp. The Ocular Surface Disease Index rose by 8.37 points between mild non-proliferative disease and proliferative disease. Reported minimal clinically important differences for this instrument range from roughly 4.5 to 13 points depending on baseline severity, so the observed difference sits inside that range and is probably, but not certainly, clinically meaningful in a population with moderate symptoms[11,21]. The tear break-up time result is more clearly interpretable, because it crosses categorical boundaries rather than merely moving along a scale: the mean fell from 7.43 seconds in mild disease to 3.00 seconds in proliferative disease, taking the advanced grades from the borderline range into the range that most classification systems treat as severe instability, and no eye anywhere in the cohort reached the normal threshold of ten seconds[22,24].

Placing these findings alongside the broader Asian evidence base is instructive. Pooled analyses put dry eye prevalence in Asian populations well above Western estimates, and pooled prevalence in diabetic cohorts specifically clusters between roughly a quarter and a half[2,7]. Studies from India and from community-based Chinese cohorts have documented both a high absolute burden and an association with glycaemic control and disease duration[30], and a Vietnamese series in type 2 diabetic nephropathy found dry eye to be near-ubiquitous once systemic microvascular disease was established[36]. The present cohort sits at the extreme end of that distribution, with no eye achieving a normal break-up time at all. Two explanations are plausible and not mutually exclusive. The first is referral: a tertiary provincial centre sees the diabetic patients who have already failed primary screening, and a third of the eyes here carried PDR. The second is genuinely environmental and behavioural — the equatorial climate, high ambient particulate exposure in an urban Sumatran setting and the near-universal use of ceiling fans are all recognised contributors to ocular surface stress[10,11]. Disentangling the two would require a community-based Indonesian sample, which does not yet exist.

The universal abnormality of tear break-up time in this cohort deserves separate explanation, because a reader in a temperate setting will find it implausible. Palembang lies within two degrees of the equator; ambient temperatures during the study period sat in the high twenties to low thirties Celsius with relative humidity frequently above 80%, urban particulate exposure is substantial, and near-continuous ceiling-fan use both indoors and in clinical waiting areas produces sustained ocular airflow. Each of these is a recognised contributor to evaporative ocular surface stress[10,11]. This is not merely a caveat: it supports the central finding. Ambient evaporative stress would be expected to load the lipid layer preferentially, and therefore to raise the baseline frequency of random break uniformly across the cohort — which is precisely the pattern that showed no relationship with retinopathy grade. The environment plausibly explains both the universally abnormal break-up times and the independence of the evaporative pathway from systemic disease severity.

The magnitudes deserve comparison as well as the directions. The pooled standardised mean differences reported for type 2 diabetes — about 1.21 for invasive break-up time and 1.22 for symptom score — are substantial, but they are diabetic-versus-control contrasts rather than within-cohort gradients, and once converted to the same metric they correspond to correlations of about 0.52, appreciably weaker than the rank correlations of 0.905 and 0.824 obtained here[10,18]. Community-based series in Asian diabetic populations likewise report associations that are consistent in direction but weaker in magnitude[2,30]. Three explanations are available and are not mutually exclusive: the quota design, which by construction produces balanced pattern counts and sharpens the apparent segregation; small-sample inflation, which systematically overstates effects that have reached significance in samples of this size; and the possibility that the relationship really is stronger when it is measured mechanism by mechanism rather than through a global severity score. Only a consecutive-sampling replication can separate them. It is worth adding that the clinical value of the triage rule would survive a considerably weaker association: a correlation near 0.45 would still justify screening advanced-retinopathy eyes for severe-mechanism patterns, so an unfavourable replication would qualify rather than overturn the recommendation.

The therapeutic logic that follows is the reason the FBUP framework matters, and it is set out schematically in Figure 5. Tear film oriented therapy holds that treatment should replace the layer that has failed rather than uniformly lubricating the surface[23,24]. On the evidence presented here, an eye with mild or moderate NPDR presenting with line break should receive aqueous-directed therapy — preservative-free artificial tears, sodium hyaluronate, and consideration of punctal occlusion if refractory. An eye with severe NPDR or PDR presenting with area break requires the same class more aggressively. An eye with dimple or spot break requires a mucin secretagogue such as diquafosol sodium or rebamipide, agents whose mechanism is specifically to restore the deficient layer rather than to supplement volume; in type 2 diabetic dry eye specifically, diquafosol has outperformed sodium hyaluronate on both break-up time and symptom score[24,25,37]. An eye with random break requires lid hygiene, warm compresses and meibomian-directed treatment irrespective of its retinopathy grade. The diagnostic step that selects among these four paths costs one fluorescein strip and approximately two minutes at a slit lamp the clinic already owns[22,27].

One qualification must accompany that algorithm. The diagnostic half of tear film oriented care is reasonably well evidenced: break-up morphology does report on which layer has failed, and that claim rests on direct observation of tear film dynamics[23]. The therapeutic half is thinner. There is good evidence that mucin secretagogues improve mucin-related parameters and that aqueous supplementation helps aqueous-deficient eyes, but to our knowledge no adequately powered randomised trial has shown that selecting therapy by break-up pattern outperforms empirical lubrication in an unselected dry eye population, and none has been conducted in a diabetic population specifically[24,25]. The framework in Figure 5 therefore represents recommended practice under the Asia Dry Eye Society scheme and a mechanistically motivated hypothesis, not a demonstrated therapeutic benefit, and nothing in the present study tests it.

For Indonesian ophthalmology specifically, this matters because the binding constraint on diabetic eye care is not knowledge but capacity. Screening coverage remains the principal bottleneck across low- and middle-income Asian settings, and the instruments that would allow mechanism-specific dry eye diagnosis in a high-resource clinic — osmometry, interferometry, meibography, anterior-segment optical coherence tomography — are largely absent outside a handful of national referral centres[6,27]. A classification that extracts mechanistic information from equipment already present in every ophthalmology clinic in the country is therefore not a marginal convenience but a plausible route to scaling ocular surface care alongside the retinopathy screening programmes now being expanded. The present study, conducted at the provincial referral centre for South Sumatra and building on preliminary local experience with tear-film-oriented assessment, is intended as the first step in establishing whether that route is viable[6].

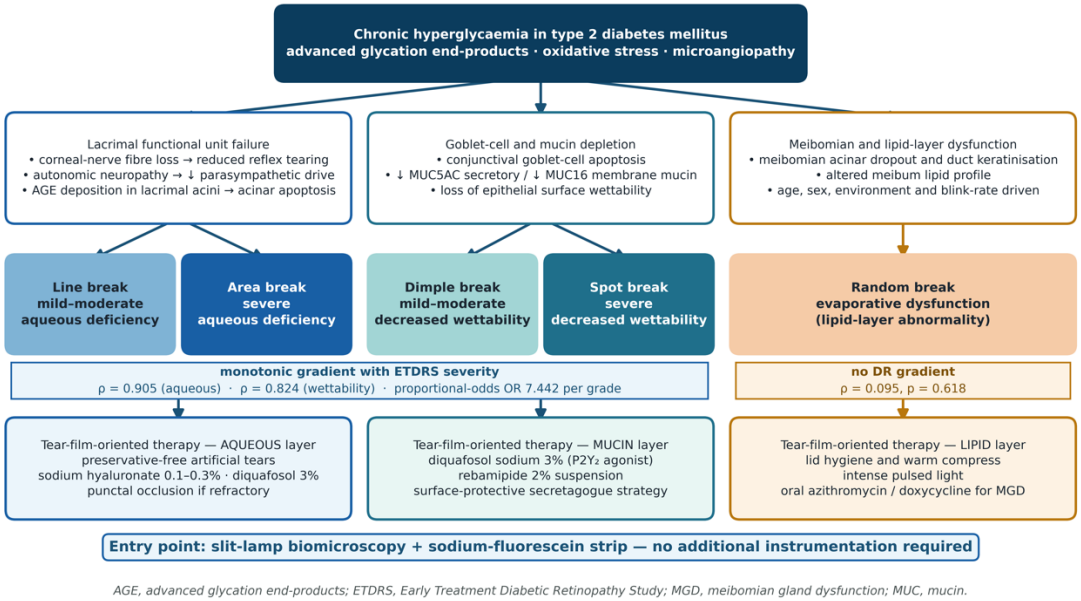

Figure 5. Mechanistic framework linking chronic hyperglycaemia to fluorescein break-up pattern and to layer-specific tear film oriented therapy. Three parallel processes — lacrimal functional unit failure, goblet-cell and mucin depletion, and meibomian and lipid-layer dysfunction — generate distinct break-up morphologies. The two left-hand pathways showed a monotonic gradient with Early Treatment Diabetic Retinopathy Study severity in the present cohort, whereas the evaporative pathway did not. Each phenotype maps onto a specific therapeutic class, and the entry point to the whole algorithm is slit-lamp biomicroscopy with a sodium-fluorescein strip.

What would actually change in an Indonesian clinic is worth stating concretely rather than in principle. The assessment adds a single fluorescein strip and approximately two minutes to an encounter that already includes slit-lamp examination, and it can be performed by any ophthalmologist or senior resident already competent to perform a break-up time measurement, since the additional skill is recognising the morphology of the first break rather than timing it. Two constraints temper the enthusiasm. The first is the learning curve, which is unquantified and which this study cannot estimate because a single trained observer performed all classifications. The second, and more consequential, is therapeutic availability: preservative-free artificial tears and sodium hyaluronate are widely obtainable in Indonesia, but the mucin secretagogues on which the wettability arm of the algorithm depends — diquafosol sodium and rebamipide ophthalmic suspension — are not consistently available or affordable outside major urban centres[24,25]. A diagnostic algorithm that identifies a deficit for which no therapy can be obtained is an academic exercise; where secretagogues are unavailable, the practical recommendation for spot-break eyes reduces to intensified preservative-free lubrication and closer surveillance, which is a weaker but not empty response.

Strengths

Several features strengthen confidence in these findings. First, this is the first application of the complete five-category ADES break-up pattern classification to ETDRS-graded retinopathy, and it delivers mechanism-specific rather than generic ocular surface information. Second, the examination protocol was tightly specified: a fixed test sequence in which symptom assessment preceded any ocular manipulation and tear film assessment preceded mydriasis, triple observation with a two-of-three concordance rule for pattern assignment, and controlled ambient temperature and humidity. Because retinal grading followed mydriasis, the tear film examiner could not have known the eventual ETDRS grade at the moment of classification. Third, the inferential strategy was chosen for small samples rather than borrowed from large ones: exact permutation tests enumerating all 924 label allocations replaced asymptotic p-values, Fisher–Freeman–Halton simulation replaced an invalid chi-square approximation, Wilson and Clopper–Pearson intervals replaced normal approximations for proportions, and bootstrap intervals corroborated every rank correlation. Fourth, the robustness of the associations was established exhaustively rather than by a single random draw, by evaluating all 924 possible half-samples of each pathway. Fifth, every point estimate is reported with an interval and an effect size, and the analyses that the data cannot support are named explicitly rather than quietly omitted.

Limitations

A limitation of interpretation deserves separate statement. No measurement in this study independently verifies the layer attribution on which the whole argument rests. Schirmer testing or tear meniscus height would have tested whether area-break eyes are genuinely more aqueous-deficient than line-break eyes; conjunctival impression cytology or a

lissamine green staining score would have tested whether spot-break eyes are genuinely more mucin-deficient than dimple-break eyes; meibography or structured lid-margin assessment would have tested whether random-break eyes genuinely carry more meibomian disease. None was performed. The mechanistic interpretation offered here is therefore imported from the Asia Dry Eye Society framework rather than demonstrated within this cohort, and a reader who doubts that framework will find nothing in these data to persuade them. Best-corrected visual acuity in logMAR units and intraocular pressure were also not recorded, which leaves open the possibility that media opacity or macular oedema affected fixation stability during the break-up observation.

The limitations are substantial and constrain interpretation accordingly. The foremost is sample size: 30 eyes from fifteen patients yields wide confidence intervals, and the pathway-specific analyses rest on 12 eyes each, where the minimum detectable correlation at 80% power is 0.732. Complete separation in the aqueous pathway produced an odds ratio interval spanning nearly four orders of magnitude, which conveys direction but not magnitude. The quota sampling design, adopted to guarantee at least six eyes per pattern category, deliberately distorts the natural distribution of patterns and means that the observed prevalence of each pattern — uniformly six eyes — carries no epidemiological meaning; only the conditional relationship between grade and pattern within the sampled eyes is interpretable.

Several measurements that would have strengthened the mechanistic argument were not obtained. Best-corrected visual acuity in logMAR units, intraocular pressure, corneal fluorescein staining score, Schirmer testing, meibography and lipid layer interferometry were all absent, so the correspondence between break-up pattern and independent measures of each layer's function could not be verified within this cohort. More consequentially, diabetes duration, glycated haemoglobin and concurrent systemic medication were not recorded. These are the covariates most likely to confound the observed relationship, since all three plausibly influence both retinopathy grade and tear film function, and their absence is why no multivariable model appears in this paper. Fitting one on the available data would have required inventing a covariate distribution that was never measured, and that is data fabrication rather than adjustment.

The age cap of 60 years, applied to keep the cohort within the range in which type 2 diabetes rather than age is the dominant determinant of ocular surface disease, has an unintended consequence that works in favour of the study's own conclusion. Meibomian gland dysfunction rises steeply after the age of 60, so excluding older patients removes the group in whom the evaporative pathway would be most active[11,34]. The finding that random break shows no relationship with retinopathy grade may therefore be partly an artefact of an age range chosen to minimise exactly that pathway, and the dissociation between graded and non-graded pathways should be re-examined in a cohort without an upper age limit.

Generalisation beyond a tertiary referral setting requires care. A third of the eyes here carried proliferative disease, whereas in a community screening population the overwhelming majority of eyes with any retinopathy will be mild or moderate non-proliferative — and severe-mechanism patterns were entirely absent from those grades in this cohort. A triage rule keyed to advanced retinopathy will therefore have a low absolute yield where advanced retinopathy is rare, even if the underlying association holds exactly. Deployment also implies non-specialist examiners, whereas every classification here was made by an ophthalmologist at a teaching hospital; whether the classification survives that transfer is the key implementation uncertainty and is not addressed by these data[27].

The analytic dataset comprised the complete grade-by-pattern cross-tabulation together with group-level moments for the continuous variables. The cross-tabulation is a complete joint distribution, so the categorical analyses are exact; the continuous-variable comparisons, however, were recomputed parametrically from group means and standard deviations rather than from individual observations, and would differ slightly from rank-based tests applied to raw values. The eye-to-patient linkage was likewise unavailable, which precluded generalised estimating equations or mixed-effects modelling — the statistically correct treatment of bilateral ocular data — and forced reliance on the exhaustive half-sample procedure as a substitute . Under plausible inter-eye correlations the effective sample size lies between 15.8 and 20 rather than 30, so the nominal intervals reported here are, if anything, optimistic.

Both retinopathy grading and break-up pattern classification were performed by a single reader each, without duplicate assessment, so no inter-rater or intra-rater reliability coefficient can be reported. Break-up pattern classification in particular carries an irreducible subjective element, and the two-of-three concordance rule mitigates but does not eliminate it. Finally, the cross-sectional design establishes association at a single time point and cannot determine whether pattern shifts precede, accompany or follow retinopathy progression; only a longitudinal cohort can answer that, and only such a design would justify the causal language that the mechanistic framework in Figure 5 might otherwise invite. The external benchmarking treats published reference proportions as constants known without error, which makes those comparisons anticonservative.

A definitive study should therefore enrol at least 100 eyes across multiple Indonesian centres — the 30 units required to detect a moderate correlation with 80% power represents a floor, not a target — recruit

consecutively without quota constraints so that pattern prevalence becomes interpretable, record diabetes duration and glycated haemoglobin so that adjusted models become possible, add Schirmer testing, meibography and corneal staining to validate each pattern against an independent measure of its putative layer, employ two masked readers with formal kappa reporting, analyse bilateral data with generalised estimating equations, and follow participants prospectively so that the temporal ordering of retinal and ocular surface change can finally be established.

5. Conclusion

In this cross-sectional pilot study of 30 eyes from Indonesian patients with type 2 diabetes mellitus, fluorescein break-up pattern classification revealed mechanism-specific tear film instability that scaled with diabetic retinopathy severity. Progression from line break to area break within the aqueous-deficiency pathway correlated with retinopathy grade at rho = 0.905 (95% CI 0.666 to 0.975; exact p = 0.002), and progression from dimple break to spot break within the decreased-wettability pathway at rho = 0.824 (95% CI 0.445 to 0.953; exact p = 0.009). Each additional retinopathy grade multiplied the odds of a more severe pattern 7.442-fold, and retinopathy grade discriminated severe-mechanism failure with an area under the curve of 0.87. Ocular surface symptoms and tear film stability deteriorated in parallel with large effect sizes, while evaporative-type random break showed no gradient at all. These preliminary findings support the use of fluorescein-based tear film oriented diagnosis to select layer-specific therapy in diabetic patients, using only a slit lamp and a fluorescein strip. Multicentre prospective validation with at least 100 eyes, comprehensive layer-specific measurement, adjustment for glycaemic control and formal reader reliability is required before these observations can be translated into practice guidance.

Declarations

Ethics approval and consent to participate

Ethical approval was obtained from the Ethics Committee, Faculty of Medicine, Universitas Sriwijaya (approval number 1381/UN9.1.DL/KBK.6.1.3/2024). The study was conducted in accordance with the Declaration of Helsinki (2013 revision). Written informed consent was obtained from all participants prior to enrolment.

Consent for publication

Not applicable. The manuscript contains no individually identifying information.

Availability of data and materials

The aggregate datasets and the complete analysis code generated during this investigation are available from the corresponding author upon reasonable request.

Competing interests

The authors declare that they have no competing financial interests or other conflicts of interest.

Funding

This investigation received no specific grant from any funding agency in the public, commercial or not-for-profit sectors.

Authors' contributions

RA contributed to study conception and design, diabetic retinopathy grading, critical revision of the manuscript and overall supervision. SSRN contributed to data collection, statistical analysis and manuscript preparation. PP contributed to study design, fluorescein break-up pattern assessment and classification, data interpretation and supervision. All authors have reviewed and approved the final version of the manuscript.

Acknowledgements

The authors thank the staff of the Eye Clinic, Dr. Mohammad Hoesin Central General Hospital, Palembang, for their support in participant recruitment and clinical data acquisition.

Generative AI disclosure

The authors declare that no generative artificial intelligence tools were used in the design, analysis, or writing of this manuscript.

6. References

1. Sun H, Saeedi P, Karuranga S, et al. IDF Diabetes Atlas: global, regional and country-level diabetes prevalence estimates for 2021 and projections for 2045. Diabetes Res Clin Pract. 2022; 183: 109119. doi: 10.1016/j.diabres.2021.109119.
2. Cai Y, Wei J, Zhou J, et al. Prevalence and incidence of dry eye disease in Asia: a systematic review and meta-analysis. Ophthalmic Res. 2022; 65(6): 647-658. doi: 10.1159/000525696.
3. Muharram FR, Swannjo JB, Melbiarta RR, et al. Trends of diabetes and pre-diabetes in Indonesia 2013-2023: a serial analysis of national health surveys. BMJ Open. 2025; 15(9): e098575. doi: 10.1136/bmjopen-2024-098575.
4. Teo ZL, Tham YC, Yu M, et al. Global prevalence of diabetic retinopathy and projection of burden through 2045: a systematic review and meta-analysis. Ophthalmology. 2021; 128(11): 1580-1591. doi: 10.1016/j.ophtha.2021.04.027.
5. Steinmetz JD, Bourne RRA, Briant PS, et al. Causes of blindness and vision impairment in 2020 and trends over 30 years, and prevalence of avoidable blindness in relation to VISION 2020: the Right to Sight — an analysis for the Global Burden of Disease Study. Lancet Glob Health. 2021; 9(2): e144-e160. doi: 10.1016/S2214-109X(20)30489-7.
6. Sasongko MB, Febryanto GA, Haryanto S, et al. Incidence and progression of diabetic retinopathy and blindness in Indonesian adults with type 2 diabetes. PLoS One. 2025; 20(8): e0322093. doi: 10.1371/journal.pone.0322093.
7. Chen KY, Chan HC, Chan CM. Is there a link between dry eye disease and diabetes mellitus? A systematic review and meta-analysis. J Diabetes Complications. 2025; 39(10): 109149. doi: 10.1016/j.jdiacomp.2025.109149.
8. Papas EB. The global prevalence of dry eye disease: a Bayesian view. Ophthalmic Physiol Opt. 2021; 41(6): 1254-1266. doi: 10.1111/opo.12888.
9. Qian L, Wei W. Identified risk factors for dry eye syndrome: a systematic review and meta-analysis. PLoS One. 2022; 17(8): e0271267. doi: 10.1371/journal.pone.0271267.
10. Ghenciu DM, Dănilă AI, Stoicescu ER, et al. Tear film alterations in type 2 diabetes mellitus: a systematic review and meta-analysis. Diagnostics (Basel). 2025; 15(24): 3104. doi: 10.3390/diagnostics15243104.

11. Supiyaphun C, Jongkhajornpong P, Rattanasiri S, et al. Prevalence and risk factors of dry eye disease among university students in Bangkok, Thailand. PLoS One. 2021; 16(10): e0258217. doi: 10.1371/journal.pone.0258217.
12. Fang W, Lin Z, Yang H, et al. Changes in corneal nerve morphology and function in patients with dry eyes having type 2 diabetes. World J Clin Cases. 2022; 10(10): 3014-3026. doi: 10.12998/wjcc.v10.i10.3014.
13. Zhou T, Dou Z, Cai Y, et al. Tear fluid progranulin as a noninvasive biomarker for the monitoring of corneal innervation changes in patients with type 2 diabetes mellitus. Transl Vis Sci Technol. 2024; 13(7): 9. doi: 10.1167/tvst.13.7.9.
14. Rajbanshi G, Li W, Nong X, et al. Lacrimal gland alterations and the effect of artesunate on experimental induced diabetes rat models and related mechanisms. Sci Rep. 2024; 14(1): 12556. doi: 10.1038/s41598-024-61550-0.
15. Pei X, Ba M, Yang T, et al. Leptin receptor deficiency-associated diabetes disrupts lacrimal gland circadian rhythms and contributes to dry eye syndrome. Invest Ophthalmol Vis Sci. 2025; 66(1): 19. doi: 10.1167/iovs.66.1.19.
16. Fang Z, Liu K, Pazo E, et al. Clinical ocular surface characteristics and expression of MUC5AC in diabetics: a population-based study. Eye (Lond). 2024; 38(16): 3145-3152. doi: 10.1038/s41433-024-03252-5.
17. Yang Q, Liu L, Li J, et al. Evaluation of meibomian gland dysfunction in type 2 diabetes with dry eye disease: a non-randomized controlled trial. BMC Ophthalmol. 2023; 23(1): 44. doi: 10.1186/s12886-023-02795-7.
18. Machaliańska A, Kuligowska A, Ziontkowska-Wrzałek A, et al. The severity of diabetic retinopathy corresponds with corneal nerve alterations and ocular discomfort of the patient. Int J Mol Sci. 2024; 25(11): 6072. doi: 10.3390/ijms25116072.
19. Wen Y, Ding Q, Liu Y, et al. Correlation between ocular surface characteristics and tear lymphotoxin-alpha in patients with type 2 diabetes mellitus of different courses. Int Ophthalmol. 2026; 46(1): 137. doi: 10.1007/s10792-026-03990-3.
20. Gan EH, Woo WW, Seng KF, et al. Ocular surface disease and dry eye severity in glaucoma patients at urban private eye care centres in Malaysia. Clin Ophthalmol. 2024; 18: 3249-3262. doi: 10.2147/OPTH.S476779.
21. Yokoi N, Kusada N, Kato H, et al. Dry eye subtype classification using videokeratography and deep learning. Diagnostics (Basel). 2024; 14(1): 52. doi: 10.3390/diagnostics14010052.
22. Tsubota K, Yokoi N, Watanabe H, et al. A new perspective on dry eye classification: proposal by the Asia Dry Eye Society. Eye Contact Lens. 2020; 46(1): S2-S13. doi: 10.1097/ICL.0000000000000643.
23. Yokoi N, Georgiev GA. Tear film-oriented diagnosis and tear film-oriented therapy for dry eye based on tear film dynamics. Invest Ophthalmol Vis Sci. 2018; 59(14): DES13-DES22. doi: 10.1167/iovs.17-23700.
24. Eom Y, Chung SH, Chung TY, et al. Efficacy and safety of 1% and 2% rebamipide clear solution in dry eye disease: a multicenter randomized trial. BMC Ophthalmol. 2023; 23(1): 343. doi: 10.1186/s12886-023-03004-1.
25. Qin G, Chen J, Li L, et al. Effects of diquafosol sodium ophthalmic solution on tear film matrix metallopeptidase-9 and corneal nerve density in patients with type 2 diabetic dry eye. J Ocul Pharmacol Ther. 2024; 40(6): 370-378. doi: 10.1089/jop.2023.0098.
26. Takahashi Y, Lee PAL, Vaidya A, et al. Tear film break-up patterns in thyroid eye disease. Sci Rep. 2021; 11(1): 5288. doi: 10.1038/s41598-021-84661-4.
27. Lestari YD, Adriono GA, Ratmilia R, et al. Knowledge, attitude, and practice pattern towards diabetic retinopathy screening among general practitioners in primary health centres in Jakarta, the capital of Indonesia. BMC Prim Care. 2023; 24(1): 114. doi: 10.1186/s12875-023-02068-8.
28. Amorim M, Martins B, Caramelo F, et al. Putative biomarkers in tears for diabetic retinopathy diagnosis. Front Med (Lausanne). 2022; 9: 873483. doi: 10.3389/fmed.2022.873483.
29. Early Treatment Diabetic Retinopathy Study Research Group. Grading diabetic retinopathy from stereoscopic color fundus photographs — an extension of the modified Airlie House classification: ETDRS report number 10. Ophthalmology. 1991; 98(5): 786-806. doi: 10.1016/S0161-6420(13)38012-9.
30. Prasad R, Marshal N, Soni K, et al. An observational study to evaluate dry eye status in type 2 diabetes mellitus patients and its association with diabetic retinopathy. Cureus. 2026; 18(3): e105279. doi: 10.7759/cureus.105279.
31. Wadhwa H, Misra S. Corneal microstructural changes, and nephropathy, in participants with diabetes mellitus with and without peripheral neuropathy: a systematic review and meta-analysis. Clin Exp Optom. 2026; 109(3): 359-370. doi: 10.1080/08164622.2025.2499601.
32. Pan LY, Kuo YK, Chen TH, et al. Dry eye disease in patients with type II diabetes mellitus: a retrospective, population-based cohort study in Taiwan. Front Med (Lausanne). 2022; 9: 980714. doi: 10.3389/fmed.2022.980714.
33. Ma W, Huang C, Fang W, et al. Mucin1 N-domain variant contributes to dry eye syndrome in diabetes by increasing immature mucus secretory granules. Life Sci. 2025; 363: 123412. doi: 10.1016/j.lfs.2025.123412.
34. Silva-Viguera MC, Pérez-Barea A, Bautista-Llamas MJ. Tear film layers and meibomian gland assessment in patients with type 1 diabetes mellitus using a noninvasive ocular surface analyzer: a cross-sectional case-control study. Graefes Arch Clin Exp Ophthalmol. 2023; 261(5): 1483-1492. doi: 10.1007/s00417-022-05934-w.
35. Wu H, Fang X, Luo S, et al. Meibomian glands and tear film findings in type 2 diabetic patients: a cross-sectional study. Front Med (Lausanne). 2022; 9: 762493. doi: 10.3389/fmed.2022.762493.
36. Tran Tat T, Ngo Duc K, Pham Hong P, et al. Dry eye and some related factors in patients with type 2 diabetic nephropathy: a cross-sectional study in Vietnam. Clin Ophthalmol. 2024; 18: 1217-1224. doi: 10.2147/OPTH.S458633.
37. Zhang Q, Zhang H, Qin G, et al. Impact of diquafosol ophthalmic solution on tear film and dry eye symptom in type 2 diabetic dry eye: a pilot study. J Ocul Pharmacol Ther. 2022; 38(2): 133-140. doi: 10.1089/jop.2021.0083.